Effects of yttrium codoping on photoluminescence of erbium-doped TiO 2 films

Chu-Chi Ting, San-Yuan Chen, Wen-Feng Hsieh, and Hsin-Yi Lee

Citation: Journal of Applied Physics **90**, 5564 (2001); doi: 10.1063/1.1413490
View online: http://dx.doi.org/10.1063/1.1413490
View Table of Contents: http://scitation.aip.org/content/aip/journal/jap/90/11?ver=pdfcov
Published by the AIP Publishing

Effects of yttrium codoping on photoluminescence of erbium-doped TiO_2 films

Chu-Chi Ting and San-Yuan Chen[a)]
Department of Materials Science and Engineering, National Chiao-Tung University, Hsinchu, Taiwan 300, Republic of China

Wen-Feng Hsieh
Institute of Electro-optical Engineering, National Chiao-Tung University, Hsinchu, Taiwan 300, Republic of China

Hsin-Yi Lee
Research Division, Synchrotron Radiation Research Center, Hsinchu, Taiwan 300, Republic of China

(Received 30 October 2000; accepted for publication 27 August 2001)

$Er^{3+}-Y^{3+}$ codoped TiO_2 films were prepared on a fused silica substrate by the sol–gel process. The effect of Y^{3+} codoping on the ~1.54 μm photoluminescence (PL) properties of Er^{3+}-doped TiO_2 films are investigated. Enhancement of PL properties due to Y^{3+} codoping by a factor of 10 for intensity and of 1.5 for the full width at half maximum in comparison with the $Er^{3+}-Al^{3+}$ codoped SiO_2 system has been observed in the film annealed at $Er^{3+}:Y^{3+}:Ti^{4+}=5:30(\sim 50):100$. Extended x-ray absorption fine structure measurements show that the local chemical environment of Er^{3+} ions in the $Er^{3+}-Y^{3+}$ codoped TiO_2 films is similar to that in Er_2O_3. The average spatial distance between Er^{3+} ions is enlarged due to the partial substitution of Y^{3+} for Er^{3+} ions in the Er_2O_3-like local structure. It is believed that the more intense PL emission of the $Er^{3+}-Y^{3+}$ codoped TiO_2 films can be attributed to the better dispersion and distorted local structure of Er^{3+} ions in the TiO_2 host matrix by yttrium codoping.
[DOI: 10.1063/1.1413490]

I. INTRODUCTION

Erbium-doped planar optical waveguides have received considerable attention for use in integrated optical devices (e.g., planar optical amplifiers or up-conversion lasers)[1–3] because the intra-$4f$ transition ($^4I_{13/2}\rightarrow{}^4I_{15/2}$) of Er^{3+} ion occurs at ~154 μm which matches the lowest signal attenuation in silica-based optical fibers.[4] Furthermore, this ~1.54 μm transition wavelength exhibits characteristics of host and temperature independence due to the outer closed $5s^25p^6$ shells screening the unfilled inner $4f^{11}$ shell.[5,6]

In order to achieve high gain optical amplification in compact optoelectronic devices, a high doping concentration of Er^{3+} ions is required. Unfortunately, the emission efficiency of ~1.54 μm photoluminescence (PL) will be degraded for higher concentration Er^{3+}-doped fiber amplifiers because of the concentration quenching effect.[7–9] Several researchers have noted that codoping with other foreign ions such as Al^{3+} is effective in dispersing rare earth ions in silicate glass matrices, since Al^{3+} ions can act as a network modifier and network former, which can further induce more nonbridging oxygen in the network of SiO_2.[10–13]

Another way to enhance ~1.54 μm PL performance is to change the host material. Since TiO_2 film has a higher refraction index ($n=2.52$ for anatase phase and $n=2.76$ for rutile phase) as well as lower phonon energy ($<700\ cm^{-1}$)[14] than silica glass film, Er^{3+}-doped TiO_2-based films have potential applications in microintegrated photonic devices. However, few detailed studies have been made to investigate the role of the Er^{3+} content in the PL properties of Er^{3+}-doped TiO_2 films.[15,16]

In this article, TiO_2 was used as the host material and a Y^{3+} ion was specially selected to be codoped with Er^{3+} ions the TiO_2 matrix because Y^{3+}/Er^{3+} ions have similar ionic radii ($Y^{3+}=0.0892$ nm and $Er^{3+}=0.0881$ nm) and Y_2O_3/Er_2O_3 has nearly the same crystal structural as well as lattice constant.[17] We demonstrate that the ~1.54 μm PL properties can be enhanced 10-fold for intensity and 1.5-fold for the full width at half maximum (FWHM) in the $Er^{3+}-Y^{3+}$ codoped TiO_2 films in comparison with the $Er^{3+}-Al^{3+}$ codoped SiO_2 system. The effects of the Y^{3+} codopant on phase development and related optical properties of Er^{3+}-doped TiO_2 films are investigated. Additionally, the extended x-ray absorption fine structure (EXAFS) technique was used to measure the local chemical environment of Er^{3+} ions that strongly affect the PL properties. A possible mechanism based on crystal chemistry is proposed to elucidate the importance of the Y^{3+} codopant in promoting the dispersion of Er^{3+} ions.

II. EXPERIMENT

A. Thin films preparation

Acetic acid (HAc, Merck) and 2-methoxyethanol (MOE, Merck) with molar ratio of Ti/HAc/MOE=1/10/15 were first added to titanium isoproxide (Alfa). The yttrium acetate

[a)]Author to whom correspondence should be addressed; electronic mail: sychen@cc.nctu.edu.tw

(Alfa) solution (a mixture of methanol and ethylene glycol) and erbium acetate (Alfa) were dissolved into the titanium solution in order to process homogeneous hydrolysis and polymerization reaction. Subsequently, the $Er^{3+}-Y^{3+}$ codoped TiO_2 precursor solution was spin coated onto fused silica substrates. The as-deposited sol–gel films were first pyrolyzed under dry oxygen atmospheres at 400 °C for 30 min at a heating rate of 3 °C/min and then annealed at temperatures ranging from 600 to 1000 °C for 1 h in dry oxygen atmosphere. Multiple spin-coating processes were employed to deposit ~0.5 μm thick films. For comparison, the composition and procedure proposed by Zhou and co-workers for $Er^{3+}-Al^{3+}$ codoped SiO_2 films were also fabricated.[13,18]

B. Characterization measurements

The phase structures of films were analyzed by an x-ray diffractometer (MAC Science, M18X) using Cu $K\alpha$ radiation. Electron spin resonance (ESR) spectra were recorded using a Brüker ESR spectrometer (EMX-10) with 100 kHz field modulation. The microwave frequency was about 9.4 GHz and the samples were cooled to about 4 K. Transmission electron microscopy (TEM) (JEOL-200CX) equipped with energy-dispersive x-rays (EDX) was used to observe and analyze the phase crystallization and composition of films. The thickness of the films was measured using a surface profilmeter (Sloan, DekTak^{3}ST). The fluorescence spectra were excited by a 980 nm diode laser with power of 50 mW inclined 45° to irradiate the sample films and were recorded normally from the film using a spectrophotometer equipped with a liquid N_2-cooled Ge detector (NCSC).

Erbium L_m-edge x-ray aborption spectra were recorded at wiggler beamline S-05B at the Synchrotron Radiation Research Center (SRRC), Hsinchu, Taiwan. The electron storage ring was operated at energy of 1.3 GeV and current of 80–200 mA. A Si(111) double-crystal monochromator with a 0.5 mm entrance slit was used for energy scanning. The energy resolution, $\Delta E/E$, was about 1.9×10^{-4}. Measurements were performed at room temperature in fluorescence mode. A polycrystalline Er_2O_3 powder (Cerac, 99.9% purity) was used as a reference standard.

III. RESULTS AND DISCUSSION

The x-ray diffraction (XRD) patterns in Fig. 1 show the effect of the annealing temperature on the phase evolution of $Er^{3+}-Y^{3+}$ codoped TiO_2 films with molar ratios of 5:0:100 (sample A), 5:10:100 (sample B), and 5:30:100 (sample C) for Er^{3+}:Y^{3+}:Ti^{4+}. For comparison, a sol–gel TiO_2 film is inserted into Fig. 1(a). As the pure TiO_2 film is being annealed at 700 °C, anatase phase is observed. However, with the incorporation of 5 mol % Er^{3+} and 10 mol % Y^{3+} ions into the TiO_2 network, the XRD peaks of the TiO_2 phase become broadened, indicating that the crystallinity of the matrix host becomes poorer. Furthermore, with an increase in the doping concentration of Y^{3+} ions to 30–50 mol %, a weak broad continuum around $2\theta=\sim30.7°$ is observed, which is characteristic of an amorphous structure. When the annealing temperature exceeded 750 °C, a strong preferred (222) peak was observed [i.e., in sample C (800 °C) of Fig. 1(b)], demonstrating that a pyrochlore phase with formula of $Er_xY_{2-x}Ti_2O_7$ has developed in the TiO_2-based amorphous structure (both Y^{3+} and Er^{3+} ions in the $Er_xY_{2-x}Ti_2O_7$ phase are structurally indistinguishable).[19] Above 900 °C, in addition to the $Er_xY_{2-x}Ti_2O_7$ pyrochlore phase, the residual TiO_2-based amorphous phase recrystallizes to form a crystalline rutile phase.

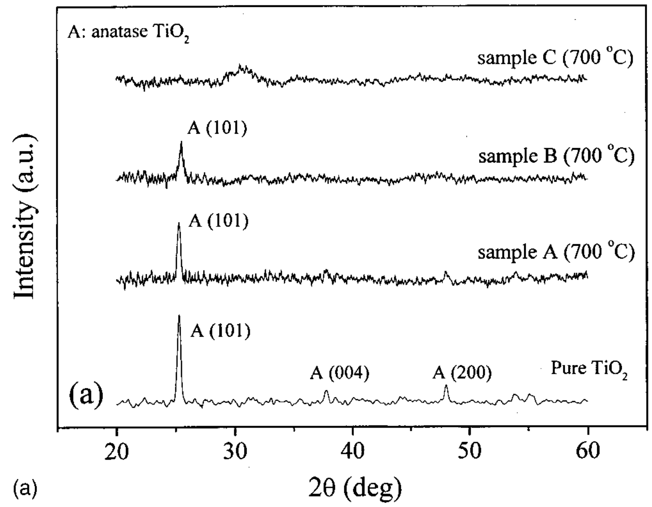

(a)

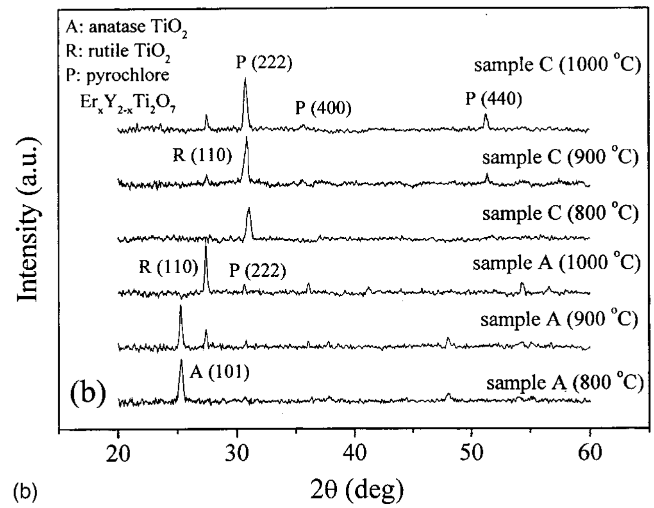

(b)

FIG. 1. XRD patterns of different $Er^{3+}-Y^{3+}$ codoped TiO_2 films annealed at (a) 700 and (b) 800–100 °C for 1 h (Er^{3+}:Y^{3+}:Ti^{4+} mole ratios for sample A=5:0:100, sample B=5:10:100, and sample C=5:30:100). Anatase TiO_2 is also shown as a reference sample.

Figure 2 shows that the refractive index (n) of the $Er^{3+}-Y^{3+}$ codoped TiO_2 films is strongly dependent on the Y^{3+}-doped concentration. An increase of Y^{3+} concentration leads to the decrease of the refractive index of the composite films. The refractive indices are 2.28, 2.25, and 2.13 at 550 nm for pure TiO_2 and $Er^{3+}-Y^{3+}$ codoped TiO_2 films (samples B and C) annealed at 700 °C for 1 h, respectively. This can be elucidated as follows. The refractive index of a heterogeneous mixture is primarily related to the refractive index and volume fraction of individual phases.[20–22] Since the refractive index of a Y_2O_3 single crystal is about 1.89, which is smaller than that ($n=2.52$ for anatase) of TiO_2, the

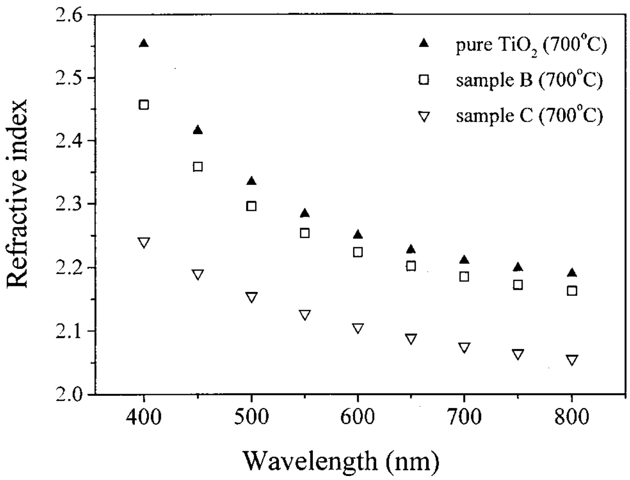

FIG. 2. Dependence of different Er^{3+}–Y^{3+} codoped TiO_2 films annealed at 700 °C for 1 h on the refractive index (Er^{3+}:Y^{3+}:Ti^{4+} mole ratios for sample B=5:10:100 and sample C=5:30:100). Anatase TiO_2 is also shown as a reference sample.

refractive indices of Er^{3+}–Y^{3+} codoped TiO_2 films should be reduced with an increase of the Y^{3+} concentration. Additionally, the refractive index of amorphous phase is lower than the highly crystalline phase (e.g., the refractive index of amorphous TiO_2 is about 2.0–2.1).[23] Therefore, a smaller and adjustable n value can be obtained for the Er^{3+}–Y^{3+} codoped TiO_2 films [see Fig. 1(a)].

The effect of the annealing temperature on the photoluminescence spectra of Er^{3+}–Y^{3+} codoped TiO_2 films (sample C) is shown in Fig. 3. When sample C was annealed below 700 °C, the PL intensity increased with increasing temperature because of the relative reduction of hydroxyl quenching centers.[9,24] On the other hand, when highly crystalline pyrochlore phase developed in the Er^{3+}–Y^{3+} codoped TiO_2 films (i.e., at annealing above 800 °C), the PL intensity was reduced and the shape of the PL spectrum obviously split into many sharp peaks. The formation of resolved manifold lines implies that the Er^{3+} ions were located on well-defined lattice sites in the $Er_xY_{2-x}Ti_2O_7$ structure. The above-mentioned phenomena are also observed for samples A and B annealed at 600–900 °C.

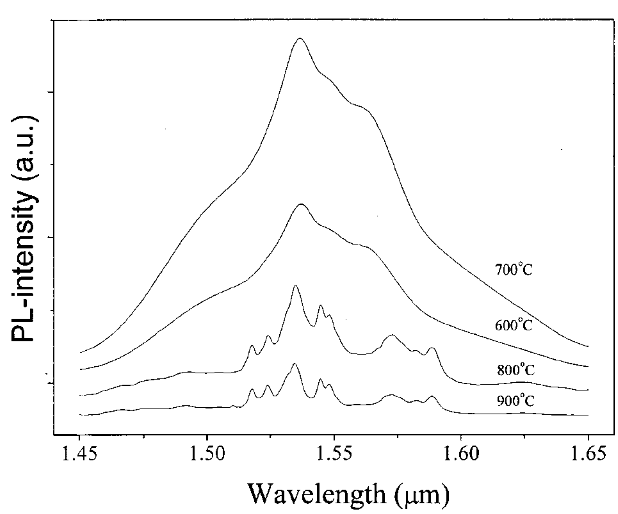

FIG. 3. Temperature dependence of the photoluminescence spectra observed from Er^{3+}–Y^{3+} codoped TiO_2 films (Er^{3+}:Y^{3+}:Ti^{4+} mole ratios for sample A=5:0:100, sample B=5:10:100, sample C=5:30:100, and sample D=10:30:100. Sample E is the Er^{3+}–Al^{3+} codoped silica film with an optimal molar ratio of (Er^{3+}:Al^{3+}:Si^{4+}=0.7:8:100). The inset is a magnified photoluminescence spectra of sample A.

The influence of Y^{3+} concentration on the photoluminescence spectra is shown in Fig. 4. A PL spectrum consisting of a sharp main peak at 1.538 μm and some side peaks at 1.506, 1.553, 1.561, and 1.579 μm is observed in the Er^{3+}-doped (5 mol %) TiO_2 films (sample A, FWHM=13 nm). However, the addition of Y^{3+} ions into the Er^{3+}-doped (5 mol %) TiO_2 films not only increases the PL intensity but also broadens the PL spectra (FWHM=36, 75, and 75 nm for samples B, C, and D, respectively). Notice that the PL spectra in samples C and D include some broad shoulders (1.502, 1.547, 1.553, and 1.562 μm) on both sides of the main peak. Such broad band emission indicates that the bonding environment of Er^{3+} ions obviously has a wider diversity with increased Y^{3+} ion concentration in Er^{3+}-doped TiO_2 films. For comparison, we also prepared Er^{3+}–Al^{3+} codoped silica films with an optimal molar ratio (Er^{3+}:Al^{3+}:Si^{4+}=0:7:8:100).[13] The PL properties of the Er^{3+}–Y^{3+} codoped TiO_2 system (sample C) exhibit more intense emission (~10-fold) and wider FWHM (~1.5-fold) than those of the optimal Er^{3+}–Al^{3+} codoped SiO_2 system. This result implies that the PL properties strongly depend on the composition and structure of the host materials. However, with increased Er^{3+} doped concentration more than or equal to 10 mol % (sample D), decreased PL intensity is observed and is attributed to the concentration quenching effect.[7–9]

The variation of the ~1.54 μm PL intensity of the Er^{3+}–Y^{3+} codoped TiO_2 films (at 700 °C) with Er^{3+} or Y^{3+} concentration is summarized in Fig. 5. By doping 1–5 mol % Er^{3+} and 10–30 mol % Y^{3+} ions into the TiO_2 host matrix, the PL intensity can be remarkably enhanced. The PL intensity of the sample [with molar ratio of Er^{3+}:Y^{3+} =5:30) is almost six times higher than that of the sample (Er^{3+}:Y^{3+}=5:10)]. However, the PL intensity does not increase more with further increases of the Y^{3+} concentration up to 50 mol %. In addition, when 10 mol % Er^{3+} ions are added (irrespective of the Y^{3+} ion concentration used), a lower PL intensity is always found (compared with the samples having 1 or 5 mol % Er^{3+} dopant). This phenomenon indicates that the concentration quenching effect occurs due to Er^{3+} ion clusters in the Er^{3+}–Y^{3+} codoped TiO_2 films. Even though more Y^{3+} ions can be incorporated into the Er^{3+}-doped TiO_2 films, there always exists a limited solid solubility of Er^{3+} ions in the distorted amorphous host matrix.

As reported in the literature, Al^{3+} ions are usually codoped in the Er^{3+}-doped SiO_2 system to reduce Er^{3+}/Er^{3+} ion clustering because it can either promote the formation of nonbridging oxygen or serve as a mutual solvent to make Er^{3+}/Er^{3+} ions soluble in the SiO_2 network.[10–13] However, in our Er^{3+}–Y^{3+} codoped TiO_2 system, no such bonding configuration ($AlO_{4/2}$ and $AlO_{6/2}$ coupled with $SiO_{4/2}$) is observed. Therefore, it is supposed that the structural model for

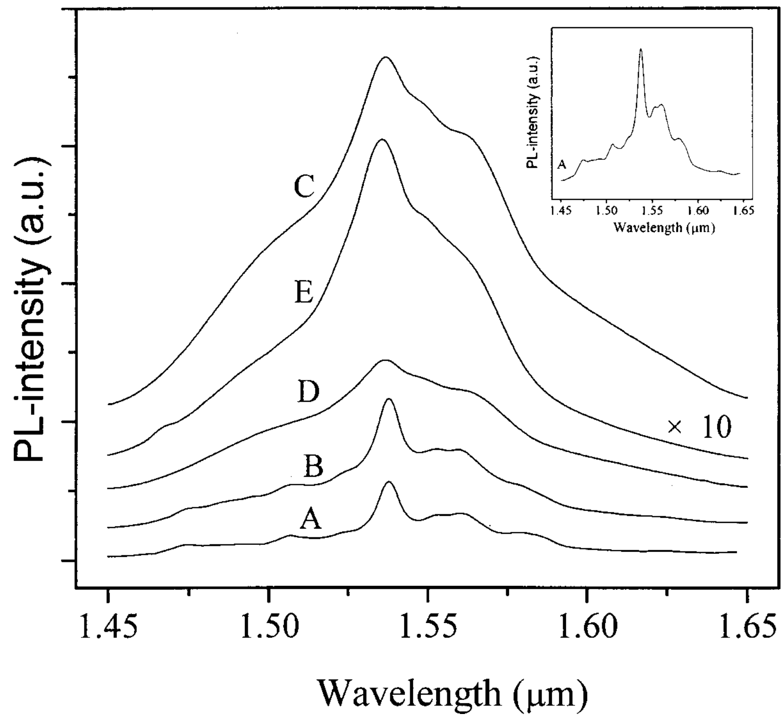

FIG. 4. ~1.54 μm PL intensity of different $Er^{3+}-Y^{3+}$ codoped TiO_2 films as a function of the Y^{3+} dose. The samples were annealed at 700 °C for 1 h.

the $Er^{3+}-Al^{3+}$ codoped SiO_2 system is not applicable to the $Er^{3+}-Y^{3+}$ codoped TiO_2 system.

It is well known that the ~1.54 μm intra-4f transition is electric dipole forbidden for the free Er^{3+} ion. If the symmetry of the local crystal field around the Er is distorted in the host materials, the parity forbidden intra-4f transition will be allowed.[25,26] However, it was generally though that for a high Er^{3+}-doped concentration, the luminescence efficiency will be reduced through energy transfer process between two nearby Er^{3+} ions (e.g., the concentration quenching effect involving cooperative upconversion or energy migration processes that result in the loss of excited ions).[7–9] That implies that the local chemical environment of Er^{3+} ions (i.e., the symmetry and clustering of Er^{3+} ions) in the host matrix significantly affects the intensity and FWHM of PL spectra. Therefore, the role of the Y^{3+} codopant in the PL properties of the Er^{3+}-doped TiO_2 films was investigated by EXAFS measurement.

Figure 6 shows the pseudoradial distribution functions obtained from the k^3-weighted Fourier transforms of the $Er^{3+}-Y^{3+}$ codoped TiO_2 films annealed at 700–800 °C for 1 h. It is observed that the Er–O bond length of the first and second nearest neighbor distances in samples A, B, and C

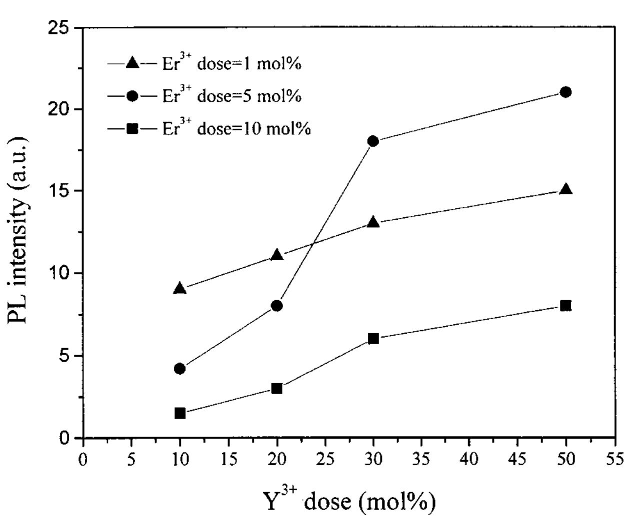

FIG. 5. Pseudoradial distribution functions obtained from the k^3-weighted Fourier transforms of different $Er^{3+}-Y^{3+}$ codoped TiO_2 films annealed at 700–800 °C for 1 (Er^{3+}:Y^{3+}:Ti^{4+} mole ratios for sample A=5:0:100, sample B=5:10:100, and sample C=5:30:100). The standard Er_2O_3 sample is also shown for comparison.

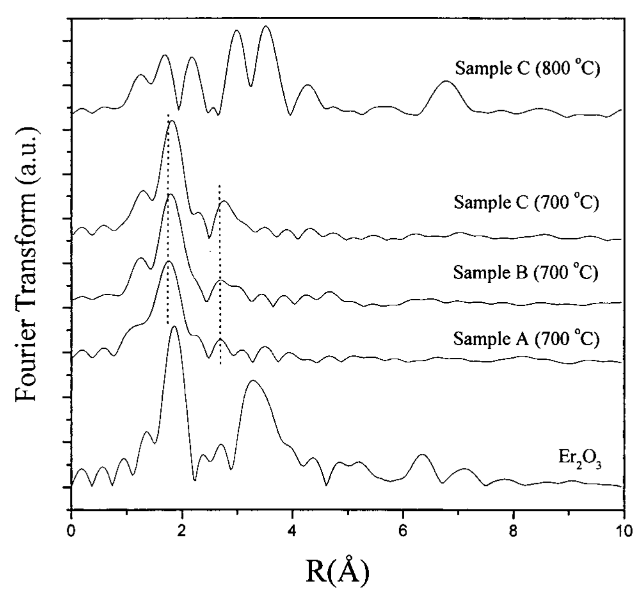

FIG. 6. ESR spectra of different $Er^{3+}-Y^{3+}$ codoped TiO_2 gel-powdered samples annealed at different temperatures for 1 h (Er^{3+}:Y^{3+}:Ti^{4+} mole ratios for sample A=5:0:100 and sample C=5:30:100).

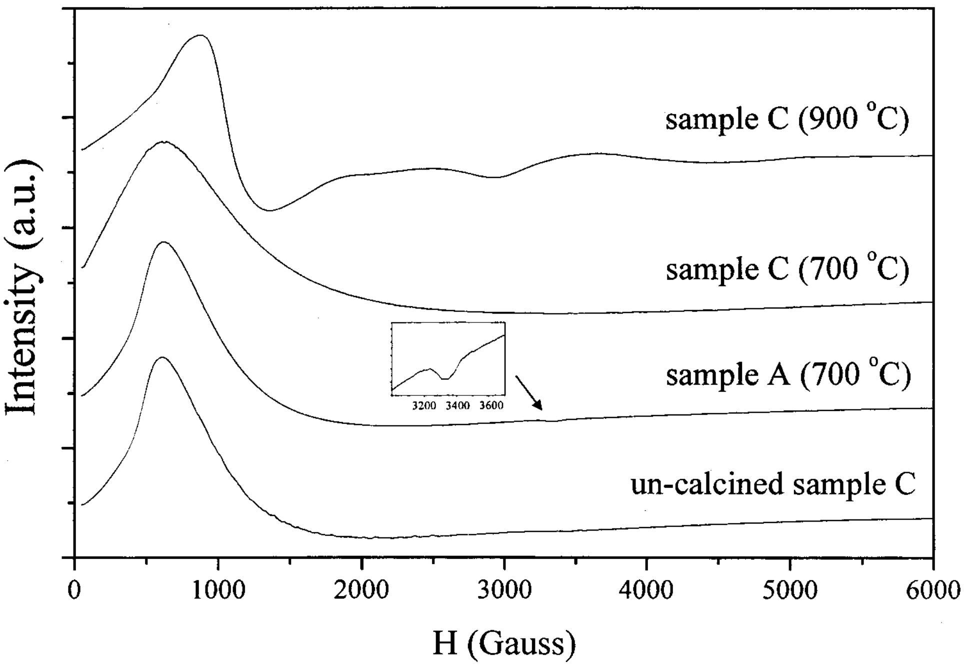

FIG. 7. ESR spectra of different $Er^{3+}-Y^{3+}$ codoped TiO_2 gel-powdered samples annealed at different temperatures for 1 h ($Er^{3+}:Y^{3+}:Ti^{4+}$ mole ratios for sample $A=5:0:100$ and sample $C=5:30:100$).

(annealed at 700 °C) is close to that of Er_2O_3. In other words, the first and second neighbor shells of Er^{3+} in the $Er^{3+}-Y^{3+}$ codoped TiO_2 films are similar to the erbium environment in the crystalline Er_2O_3. The same phenomenon has been observed in other systems such as $Er^{3+}-O^{2-}$ codoped Si and Er^{3+}-doped multicomponent glasses for which it was reported that the local chemical environment of Er^{3+} ions had an Er_2O_3-like environment (i.e., optically active centers).[27–30] However, it should be noted that the first and second neighbor distances around Er^{3+} ions gradually become enlarged with an increase of the Y^{3+} concentration from 0 to 30 mol % (see Fig. 6). Since both Er^{3+} and Y^{3+} ions have the same valences and similar ionic radii, they can be replaced with each other. Therefore, the enlarged second neighbor distance seems to reveal that the second shell may be partially a result of contributions from Y^{3+} ions because the ionic radius of the Y^{3+} ion is somewhat larger than that of the Er^{3+} ion. This will result in enlargement of the average atomic spacing among Er ions due to the partial occupancy of Y^{3+} ions on the second shell of Er^{3+} ions (e.g., the formation of Er–O–Y–O–Er bonds replaces Er–O–Er–O–Er bonds), which can reduce the concentration quenching effect and enhance the PL intensity.

In addition, the increased PL intensity is also related to the distorted local structure of Er^{3+} ions that can increase the probability of the normally forbidden intra-4f transition. As shown in Fig. 5, the Er^{3+} (5 mol %)-doped TiO_2 film exhibited a sharper PL spectrum, which means that Er^{3+} ions are located on well-defined lattice sites in the crystalline anatase TiO_2 matrix. However, with the incorporation of Y^{3+} ions into the Er^{3+}-doped (5 mol %) TiO_2 films, the intrinsic network of the TiO_2 host matrix becomes distorted and the phase evolution from a poorly crystallized anatase to an amorphous structure is observed at 700 °C annealing (see Fig. 1). Furthermore, as seen from TEM examination (not shown here), no microcrystals (such as $Er_xY_{2-x}O_3$, TiO_2, and $Er_xY_{2-x}Ti_2O_7$) were detected in the amorphous $Er^{3+}-Y^{3+}$ codoped TiO_2 films. Therefore, Er^{3+} ions would be located on the distorted sites in the amorphous $Er^{3+}-Y^{3+}$ codoped TiO_2 system and the ligand field experienced by each Er^{3+} ion is more diversified. This leads to enhanced PL intensities and Stark splitting of excited state/ground state manifolds, promoting an inhomogeneous broadening effect (as one can see in the broad PL spectra in Fig. 4).

On the other hand, when the $Er^{3+}-Y^{3+}$ codoped TiO_2 films are annealed above 800 °C, the highly crystalline $Er_xY_{2-x}Ti_2O_7$ phase forms in the host matrix and the local chemical environment of Er^{3+} ions has completely changed (as shown in Fig. 6). In the highly crystalline $Er_xY_{2-x}Ti_2O_7$ phase, the Er^{3+} ions were located on well-defined lattice sites and the coordination number of Er^{3+} ions is eightfold.[31–33] The local environment around the Er^{3+} ions becomes more uniform (or isolated) and with higher-order symmetry compared to that in the amorphous host matrix. Hence a number of sharper PL lines along with the reduced PL intensity due to the forbidden 4f transition are observed (see Fig. 3).

Although EXAFS is a powerful technique by which to study the change of the local Er^{3+} structure, ESR spectra can also shown the characteristic of the Er atom configuration that is influenced by the local chemical environment.[34,35] Figure 7 shows ESR spectra of $Er^{3+}-Y^{3+}$ codoped TiO_2 gel-powdered samples annealed at 700–900 °C. All of the samples at 700 °C exhibit a broad low-field Er^{3+}3+ signal.[36,37] According to Barrière *et al.*, the hyperfine lines of the Er ESR peak were detected only for 1 mol % Er.[38] However, in the present work, a high doping concentration of Er (5 mol %) was used. Therefore, the broad ESR peak is attributed to Er^{3+} unresolved hyperfine splitting. In the Er^{3+}-doped TiO_2 system (sample A), a relatively small peak with g value of 2 due to the contribution by Ti^{4+} ions is observed.[39] However, the addition of 30 mol % Y^{3+} ions into the Er^{3+}-doped TiO_2 system will result in broadening of the Er^{3+} ESR signal and disappearance of the Ti^{4+} ESR signal. Because sample C was annealed at 900 °C (well-crystallized rutile and pyrochlore phases form), a sharp Er^{3+} ESR signal along with other small broad peaks are observed in the ESR spectra. Note that no trace of a quenched Er^{3+} ESR signal corresponding to Er^{3+} ion clusters is detected in the $Er^{3+}-Y^{3+}$ codoped TiO_2 system. The variation of Er^{3+} ESR signals in the $Er^{3+}-Y^{3+}$ codoped TiO_2 system again reveals that yttrium codoping and annealing temperatures (about 800 °C) obviously affect the local chemical environment of Er^{3+} ions, which reflects the difference in PL properties among different samples.

Therefore, it is believed that the improved ~1.54 μm PL performance of the $Er^{3+}-Y^{3+}$ codoped TiO_2 films can be attributed to the better dispersion and the distorted local structure of Er^{3+} ions in the amorphous host matrix.

IV. CONCLUSION

An enhancement of ~1.54 μm in PL properties due to Y^{3+} codoping effects was obtained from $Er^{3+}-Y^{3+}$ codoped TiO_2 films annealed at 700 °C with molar ratio of $Er^{3+}:Y^{3+}:Ti^{4+}=5:30(\sim 50):100$. It is believed that the local chemical environment of Er^{3+} ions in $Er^{3+}-Y^{3+}$ codoped TiO_2 films is similar to that in Er_2O_3. Furthermore, the average spatial distance between Er^{3+} ions is enlarged due to the partial substitution of Y^{3+} for Er^{3+} ions in the Er_2O_3-like local structure. Therefore, the enhanced PL intensity can be attributed to contributions by the increased dispersion and distorted local structure of Er^{3+} ions in $Er^{3+}-Y^{3+}$ codoped TiO_2 films. We believe that the low fabrication temperature and the high efficiency/wide bandwidth of the PL properties for $Er^{3+}-Y^{3+}$ codoped TiO_2 films may open up another new possible way to fabricate planar waveguide amplifiers in integrated optics.

ACKNOWLEDGMENTS

The authors would like to thank Professor Y. C. Lia and R. Mong for helpful discussion and for PL measurements. Dr. J. F. Lee of the Synchrotron Radiation Research Center is also thanked for the EXAFS measurement and analysis. This work was financially supported by the National Science Council of the Republic of China, Taiwan, under Contract No. NSC89-2216-E-009-034.

[1] T. Kitagawa, K. Hattori, M. Shimizu, Y. Ohmori, and M. Kobayashi, Electron. Lett. **27**, 334 (1991).
[2] G. Nykolak, M. Haner, P. C. Becker, J. Shmulovich, and Y. H. Wong, IEEE Photonics Technol. Lett. **5**, 1014 (1993).
[3] T. Feuchter, E. K. Mwarania, J. Wang, L. Reekie, and J. S. Wilkinson, IEEE Photonics Technol. Lett. **4**, 1818 (1992).
[4] T. Miya, Y. Terunuma, T. Hosaka, and T. Miyashita, Electron. Lett. **15**, 106 (1979).
[5] H. Ennen, J. Schneider, G. Pomrenke, and A. Axmann, Appl. Phys. Lett. **43**, 943 (1983).
[6] H. Ennen, G. Pomrenke, A. Axmann, K. Eisele, W. Haydl, and J. Schneider, Appl. Phys. Lett. **46**, 381 (1985).
[7] O. Lumholt, T. Rasmissen, and A. Bjarklev, Electron. Lett. **29**, 495 (1993).
[8] P. Blixt, J. Nilsson, T. Carlnäs, and B. Jaskorzynska, IEEE Photonics Technol. Lett. **3**, 996 (1991).
[9] Y. Yan, A. J. Faber, and H. de Waal, J. Non-Cryst. Solids **181**, 283 (1995).
[10] K. Arai, H. Namikawa, K. Kumata, T. Honda, Y. Ishii, and T. Handa, J. Appl. Phys. **59**, 3430 (1986).
[11] C. K. Ryu, H. Choi, and K. Kim, Appl. Phys. Lett. **66**, 2496 (1995).
[12] B. J. Ainslie, S. P. Craig, and S. T. Davey, Mater. Lett. **5**, 143 (1987).
[13] Y. Zhou, Y. L. Lam, S. S. Wang, H. L. Liu, C. H. Kam, and Y. C. Chan, Appl. Phys. Lett. **71**, 587 (1997).
[14] C. Urlacher and J. Mugnier, J. Raman Spectrosc. **27**, 785 (1996).
[15] A. Bahtat, M. Bouazaoui, M. Bahtat, and J. Mugnier, Opt. Commun. **111**, 55 (1994).
[16] A. Bahtat, M. Bouderbala, M. Bahtat, M. Bouazaoui, J. Mugnier, and M. Druetta, Thin Solid Films **323**, 59 (1998).
[17] ASTM JCPDS File Nos. 08-0050 (Er_2O_3) and 25-1200 (Y_2O_3) (1997).
[18] Q. Xiang, Y. Zhou, Y. L. Lam, Y. C. Chan, and C. H. Kam, Ferroelectrics **230**, 357 (1999).
[19] ASTM JCPDS File Nos. 18-0499 ($Er_2Ti_2O_7$) and 18-1475 ($Y_2Ti_2O_7$) (1997).
[20] D. E. Aspnes, Am. J. Phys. **50**, 704 (1982).
[21] D. E. Aspnes, Thin Solid Films **89**, 249 (1982).
[22] A. Feldman, Proc. SPIE **821**, 129 (1987).
[23] B. E. Yoldas, Appl. Opt. **21**, 2960 (1982).
[24] O. Chauvet and L. Forro, Solid State Commun. **93**, 667 (1995).
[25] B. R. Judd, Phys. Rev. **127**, 750 (1962).
[26] R. M. Moon, W. C. Koehler, H. R. Child, and L. J. Raubenheimer, Phys. Rev. **176**, 722 (1968).
[27] P. M. Peters and S. N. Houde-Walter, J. Non-Cryst. Solids **239**, 162 (1998).
[28] D. L. Adler, D. C. Jacobson, D. J. Eaglesham, M. A. Marcus, J. L. Benton, J. M. Poate, and P. H. Citrin, Appl. Phys. Lett. **61**, 2181 (1992).
[29] A. Terrasi, G. Franzò, S. Coffa, F. Priolo, F. D'Acapito, and S. Mobilio, Appl. Phys. Lett. **70**, 1712 (1992).
[30] M. Ishii, T. Ishikawa, T. Ueki, S. Komuro, T. Morikawa, Y. Aoyagi, and H. Oyanagi, J. Appl. Phys. **85**, 4024 (1999).
[31] M. A. Subramanian, G. Aravamudan, and G. V. Subba Rao, Prog. Solid State Chem. **15**, 55 (1983).
[32] J. M. Longo, P. M. Raccah, and J. B. Goodenough, MRS Bull. **4**, 191 (1969).
[33] H. S. Horowitz, J. M. Longo, and J. T. Lewandowski, MRS Bull. **16**, 489 (1981).
[34] J. D. Carey, R. C. Barklie, J. F. Donegan, F. Priolo, G. Franzò, and S. Coffa, J. Lumin. **80**, 297 (1999).
[35] T. Ishiyama, E. Katayama, K. Murakami, K. Takahei, and A. Taguchi, J. Appl. Phys. **84**, 6782 (1998).
[36] K. Kojima, S. Yoshida, H. Shiraishi, and A. Maegawa, Appl. Phys. Lett. **67**, 3423 (1995).
[37] M. Yamazaki and K. Kojima, J. Mater. Sci. Lett. **14**, 813 (1995).
[38] A. S. Barrière, T. Césaire, L. Hirsch, B. Porté, G. Villenueve, L. Lezama, T. Rojo, and G. E. Barberis, J. Appl. Phys. **84**, 3654 (1998).
[39] O. Chauvet, L. Forro, I. Kos, and M. Miljak, Solid State Commun. **93**, 667 (1995).